Missing rainfall extremes in CML data due to total loss of signal

Julius Polz[1], **Maximilian Graf**[1], **Christian Chwala**[1,2]

[1]Institute of Meteorology and Climate Research, Karlsruhe Institute of Technology, Campus Alpin, Garmisch-Partenkirchen, Germany
[2]Chair of Regional Climate and Hydrology, Institute of Geography, University of Augsburg, Augsburg, Germany

Key Points:

- Total loss of commercial microwave link signals during heavy rain leads to missing rainfall extremes
- Magnitude of observed blackouts exceeds climatologically expected values
- Unexpectedly, longer CMLs experience more blackouts

Corresponding author: Julius Polz, julius.polz@kit.edu

Corresponding author: Maximilian Graf, maximilian.graf@kit.edu

Abstract

An important aspect of rainfall estimation is to accurately capture extreme events. Commercial microwave links (CMLs) can complement weather radar and rain gauge data by estimating path-averaged rainfall intensities near ground. Our aim with this paper was to investigate attenuation induced total loss of signal (blackout) in the CML data. This effect can occur during heavy rain events and leads to missing extreme values. We analyzed three years of attenuation data from 4000 CMLs in Germany and compared it to a weather radar derived attenuation climatology covering 20 years. We observed on average twelve times more blackouts in the CML data than we would have expected from the radar derived climatology. Blackouts did occur more often for long CMLs, which was an unexpected finding. In conclusion, both the hydrometeorological community and network providers can consider our analysis to develop mitigation measures.

Plain Language Summary

Commercial microwave links (CMLs) are used to transmit information between towers of cellphone networks. If there is rainfall along the transmission path, the signal level is attenuated. By comparing the transmitted and received signal levels, the average rainfall intensity along the path can be estimated. If the attenuation is too strong, no signal is received, no information can be transmitted and no rainfall estimate is available. This is unfavorable both for network stability and rainfall estimation. In this study, we investigated the frequency of such blackouts in Germany. How many blackouts per year are observed in a three year CML dataset covering around 4000 link paths and how many are expected from 20 years of weather radar data? We observed on average twelve times more blackouts in the CML data than we expected from the radar derived climatology. Blackouts did occur more often for long CMLs, which was an unexpected finding. While only one percent of the annual rainfall amount is missed during blackouts, the probability that a blackout occurs was very high for high rain rates. Both, the hydrometeorological community and network providers can consider our analysis to develop mitigation measures.

1 Introduction

Microwave radiation is attenuated by hydrometeors through scattering and absorption processes. For raindrops an advantageous relationship between specific attenuation k in dB/km and rainfall rate R in mm/h exists. This power law known as the k-R relation is close to linear at frequencies between 20 and 35 GHz (Chwala & Kunstmann, 2019). Commercial microwave links (CMLs) use frequencies from 7 to 80 GHz and thus can be used to derive path averaged rainfall intensities by comparing transmitted and received signal levels (TSL and RSL) (Uijlenhoet et al., 2018). In theory, the k-R relation is valid for arbitrary rainfall intensities occurring in the underlying drop size distribution simulations. In practice, the measurement of high attenuation values at a given transmitted signal level has an upper bound when the signal cannot be distinguished from the receiver's background noise.

CML rainfall estimates were derived for many countries around the globe, e.g. country-wide rainfall estimates from the Netherlands (Overeem et al., 2016), Sri Lanka (Overeem et al., 2021), and Germany (Graf et al., 2020). CML-derived rainfall information can be used for applications like streamflow prediction, urban drainage modeling, agricultural purposes and rainfall nowcasting (Fencl et al., 2013; Smiatek et al., 2017; Stransky et al., 2018; Imhoff et al., 2020). Especially for flash flood prediction, precise precipitation maxima are of great importance (Cristiano et al., 2017). While rainfall estimates from weather radars are known to underestimate high intensities (Schleiss et al., 2020), rain gauges lack spatial representativeness (Sevruk, 2006). CMLs can fill this information gap by estimating path averaged intensities at path lengths of a few kilometres.

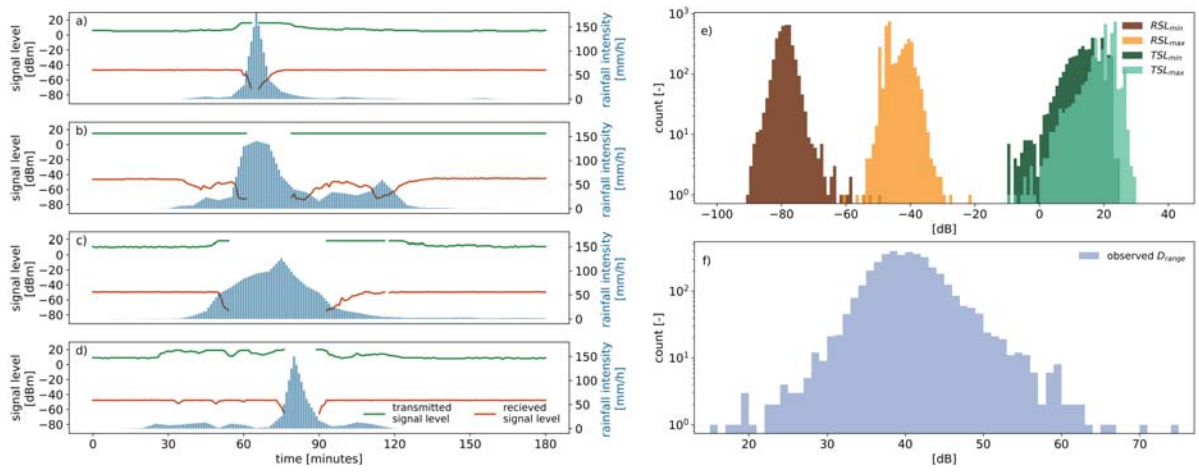

Figure 1. a)-d) show TSL and RSL time series during blackout gaps from four CMLs. Rainfall intensities are derived from RADKLIM-YW along the CML's paths. e) gives the minimal and maximal TSL and RSL values of all 3904 CMLs for the analysed period of three years. f) shows the distribution of the dynamic range directly calculated from CML signal levels with Equation 1.

Recent studies on the quality of CML rainfall estimates suggest a good agreement with radar and rain gauge estimates (Graf et al., 2021; Overeem et al., 2021). However, missing periods in the signal level time series might be excluded e.g. when comparing CML time series against a path-averaged radar reference or rain gauges. Such periods can occur due to hardware failure, maintenance or outages in the data acquisition. Additionally, network providers usually design the hardware in such a way that transmission outages due to high attenuation (blackouts) are allowed to occur for a certain amount of time per year. The International Telecommunication Union (ITU) recommends a minimum availability of 99.99% which would allow up to 52 minutes of total loss of signal per year (ITU-R, 2017).

Rainfall is the prevalent reason for CML signal attenuation. Hence, the amount of missing data is in a close relationship with the local rainfall climatology. Because of blackouts rainfall estimates from CMLs miss peak intensities, an error which propagates to further applications. Figure 1 shows examples of such blackouts in CML attenuation time series and the rainfall intensity according to a weather radar reference. To date, it is unclear to which extent rain events are missed due to blackouts.

Our aim is to answer two questions related to CML blackouts using a country-wide CML network in Germany. The first question is how many blackouts each CML is experiencing in practice and how this affects rainfall estimates. The second question is how much blackout time is expected considering 20 years of high-resolution weather radar rainfall climatology and whether this expectation is met in practice.

2 Data and Methods

Our analysis was based on observed blackouts within CML data collected in Germany and a comparison to the expected frequency derived from weather radar climatology (Sec. 2.1). We detected gaps in CML data that are assumed to be caused by attenuation (Sec. 2.2) and derived path integrated attenuation values from path averaged weather radar rain rates (Sec. 2.3). Note that all calculations were repeated for each CML individually.

2.1 Data

CML data has been collected in cooperation with Ericsson Germany. The data acquisition system described by (Chwala et al., 2016) has been used to record three years of instantaneously measured RSL and TSL of 3904 CMLs distributed over Germany (2018 to 2020). The temporal resolution is one minute and the power resolution is 0.3 or 0.4 dBm for RSL and 1 dBm for TSL. 25% of the CMLs have a constant TSL value (e.g. Figure 1b). The other 75% use an automatic transmit power control (ATPC), which can increase TSL (e.g. Figure 1a,c,d). The CML path lengths range from 0.1 to 30 kilometers with frequencies from 7 to 40 GHz as shown in Figure 2d). In the context of rainfall estimation, CMLs are characterized by two main features. First, the signal level sensitivity to rainfall, see e.g. Fig. 7 in Chwala and Kunstmann (2019), which depends on the frequency, polarization and path length. Second, the dynamic range of the signal level D_{range}, i.e. the difference between clear sky attenuation and maximum measurable attenuation. The communication along a CML requires (de-)modulation of information onto the carrier frequency. If the RSL is too low, i.e. close to the noise floor of the receiver, the error rate for demodulation becomes too large and communication is cut off. Datasheets of CML hardware (e.g. from Ericsson (2012)) guarantee a certain error rate at defined low RSL values rather than a fixed lower RSL limit where this cutoff happens. Therefore, we need to estimate the empirical D_{range} of each CML as

$$D_{range} = TSL_{max} - RSL_{min} - TSL_{min} + RSL_{max}. \tag{1}$$

We removed TSL and RSL outliers outside the intervals [-20 dBm, 50 dBm] and [-99 dBm, 0 dBm] respectively. TSL_{max} and RSL_{min} were the single lowest (highest) value which occurred occasionally during heavy attenuation events. We assumed that TSL_{min} and RSL_{max} are occurring frequently during clear sky conditions. We used the 99.995% quantiles of TSL as minimum and of RSL as maximum to avoid that outliers distort D_{range}. With the potentially abrupt onset of heavy rainfall causing a complete loss of signal, RSL_{min} may have been undersampled. Therefore, D_{range} is assumed to be the minimal dynamic range a CML can be expected to have.

As reference we used RADKLIM-YW (Winterrath et al., 2018) from the German Meteorological Service (DWD) which we linearly interpolated from a 5- to a 1-minute resolution to match the CML resolution. RADKLIM-YW is a gauge-adjusted, climatologically corrected radar product with a temporal resolution of five minutes and a spatial resolution of 1 km. The underlying radar precipitation scans have been carried out every five minutes. Therefore, the radar rainfall intensities can be considered to be instantaneous measurements without temporal averaging. The product is composed of 17 weather radars and adjusted by more than 1000 rain gauges with additive and multiplicative corrections. The climatological correction accounts for range-dependent underestimation and radar spokes caused by beam blockage, among others. RADKLIM-YW was considered the best and highest resolved rainfall reference for this analysis and was available from 2001 to 2020. Following Graf et al. (2020) we derived the path averaged rain rate R for each CML as the sum of radar grid cell rainfall intensities r_i weighted by their lengths of intersection l_i with a given CML path of total length L as described by Eq. 2.

$$R = 1/L \sum_i r_i l_i \tag{2}$$

2.2 Detecting blackouts in CML data

Gaps in CML signal level time series can have various reasons. In this analysis we were interested in gaps caused by strong attenuation during heavy rainfall and therefore excluded periods which could be attributed to one of the following reasons. Gaps longer

than 24 hours were assumed not to be caused by heavy rain events. When more than 400 CMLs exhibited a gap at the same time, we assumed a partial or complete outage of our data acquisition system and excluded the timestep. Gaps occurring during a period where a seven day rolling mean of the RSL was below -60 dBm were removed. For these periods we assumed that there is a long term transmission disturbance, i.e. partial beam blockage, since none of the CMLs in our dataset has a 3 year median RSL below -60 dBm. Around 0.2% of all RSL values are removed from the analysis by these filters.

In the remaining CML data, gaps are identified as blackouts if either the last valid RSL before, or the first valid RSL after this gap was below -65 dBm. Examples of such automatically detected gaps are shown in Figure 1a-d). We chose a threshold at -65 dBm to separate it from the median RSL levels, which are above -60 dBm for all CMLs in our dataset. However, this threshold might need adjustment if our method is applied for CML datasets with different characteristics.

We grouped observed blackouts into reference rainfall intensity bins and computed the average amount of observed blackout minutes n_{obs} per year for each CML. In addition, n_{obs} was normalized by applying the factor

$$f_{avail} = \frac{\#\{\ minutes\ in\ observation\ period\}}{\#\{\ minutes\ with\ valid\ observations\}} \tag{3}$$

for each CML to account for missing timesteps in the CML data.

2.3 Deriving a blackout climatology from radar data

In theory, a blackout due to heavy rainfall should be expected, whenever the path integrated attenuation (PIA) exceeds the CML's dynamic range D_{range}. We estimated a blackout climatology using 20 years of instantaneous radar measurements. A radar derived PIA was calculated by individually applying the k-R relation to the rain rate r_i of the i-th radar grid cell intersected by a CML path. This procedure was chosen over applying the k-R relation to the path averaged rain rate to minimize errors due to the spatial variability of rainfall along the path as explored by Berne and Uijlenhoet (2007). Hence, we calculate

$$PIA = 1/L \sum_i a r_i^b l_i + w_{aa} \tag{4}$$

using coefficients a and b, derived from the ITU recommendation ITU-R (2005), which depend on the CMLs frequency and polarization. The intersection length of CML path and radar grid cell i is denoted l_i. Additionally, a constant w_{aa} =3 dB accounting for the wet antenna attenuation (WAA) caused by rain drops on the cover of the CML antennas was added (van Leth et al., 2018). We chose a value similar to Leijnse et al. (2008); Schleiss et al. (2013). We assumed a high constant value which is reasonable for peak rainfall intensities. Whenever PIA was larger than D_{range}, the CML was expected to show a blackout gap. Thus, we derived the cumulative amount of expected blackout minutes $n_{ex}(D_{range})$ as the average amount of timestamps per year where PIA$> D_{range}$ multiplied by five due to the radar's instantaneous sampling rate of five minutes. We applied Eq. 3 to n_{ex} according to the radar availability along CML paths. Due to RSL_{min} undersampling, D_{range} might be higher in reality than estimated. In turn, n_{ex} should be lower than estimated, i.e. we would expect n_{obs} to be smaller than n_{ex}.

3 Results

3.1 CML signal levels and dynamic ranges

The distribution of TSL_{min} and TSL_{max} is defined by hardware configuration. The distribution of RSL_{min} and RSL_{max} depends on TSL, path length and path loss. The

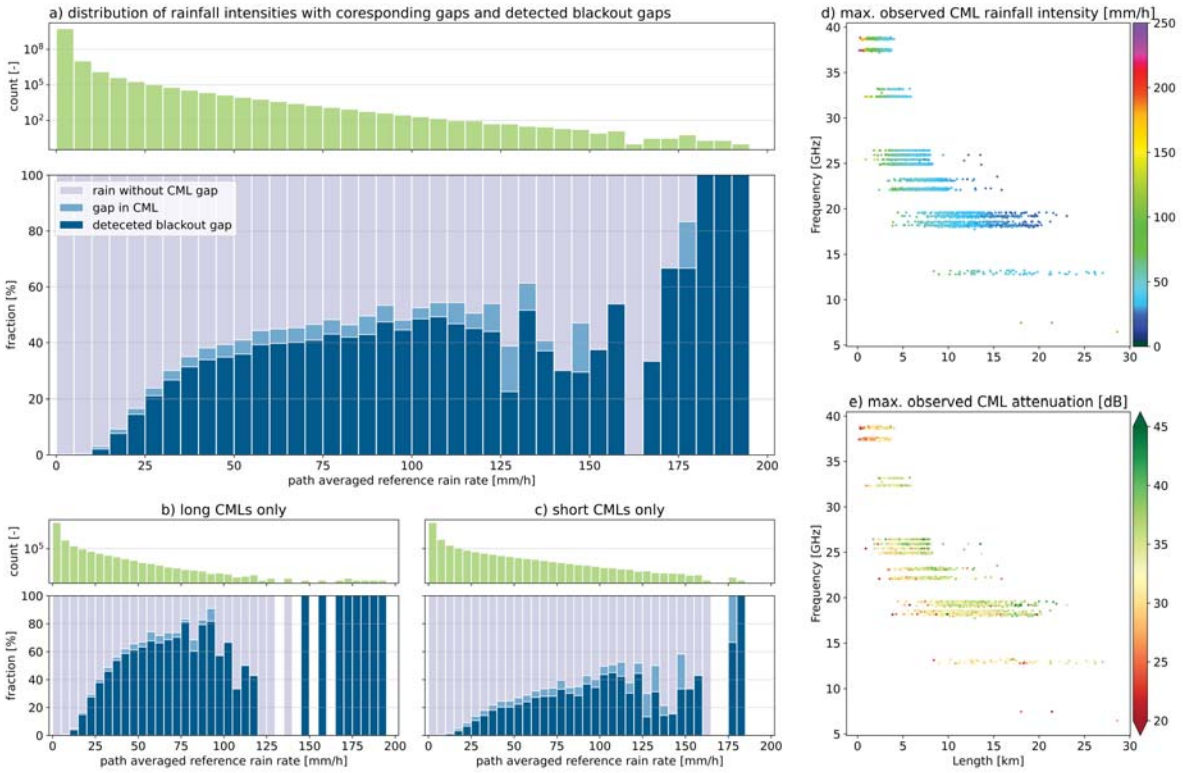

Figure 2. a) shows the distribution of the reference rainfall intensities in green. For each bin the fraction of gaps in the CMLs RSL time series and the fraction of the detected blackout gaps are shown in light and dark blue. b) and c) show the same for the longest and shortest quartile of all CMLs, respectively. d) shows the maximal rainfall intensity derived from the CMLs estimated with the rainfall retrieval methodology from Graf et al. (2020) and Polz et al. (2020). e) shows the respective maximal attenuation observed at each CML during the analysed three years.

spread of observed RSL_{max} is lower than the spread of observed RSL_{min}. The distribution of the dynamic range estimate is shown in Figure 1f). The observed D_{range} was on average 40.5 dB with a minimum of 15.2 dB and a maximum of 74.3 dB.

3.2 Observed CML blackout gaps

Figure 2a) shows a histogram of path-averaged radar rainfall intensities. The higher the path-averaged rainfall intensity the less frequently it occurred. For each bin the fraction of CML data gaps which were detected as blackout gaps are shown (dark blue). In addition, the fraction of all gaps that have not been detected as blackout are shown (light blue). Note that gaps that were attributed to, e.g. failure of the data acquisition, have been removed. The fraction of gaps is increasing quickly until 50 mm/h and then less steep up to 125 mm/h. For very high intensities above 125 mm/h the sample size was less than 50 minutes per bin. Therefore, the fraction of all gaps, including detected blackout gaps, was getting sensitive to the occurrence of individual events and hence the statistics were less robust. Overall, around 95% of the gaps during rainfall in the radar reference were detected as blackout gaps. This fraction varied for the highest observed rainfall intensities due to the small sample size. Based on the statistics from Figure 2a), CMLs missed on average 1% of the yearly rainfall sum during blackout gaps.

The quartile of long CMLs in 2b) showed a higher fraction of (blackout) gaps. Additionally, path-averaged rainfall intensities are lower on average as longer paths average out peak intensities. The quartile of short CMLs shows less (blackout) gaps and higher rainfall intensities. This pattern is also visible in 2d) and e) where the maximum instantaneous rainfall intensity and attenuation from each CMLs observations are shown. While the maximum attenuation increased with length, the maximum observed path-averaged rainfall intensity decreased. The maximum observed rainfall intensity from CMLs with 600 mm/h (and several events above 250 mm/h all beyond the figures colorscale) is well above the maximum intensity of the path averaged reference product. Overall, shorter CMLs show less blackouts during heavy rainfall.

3.3 Expected blackout gaps derived from radar based attenuation climatology

Expected PIA values along each CML path were derived using Equation 4 and 20 years of RADKLIM-YW data. Figure 3 shows path-averaged rain rate and PIA percentiles corresponding to the highest 60, five or one minutes per year and the 20-year maximum for individual CMLs. The expected PIA was increasing with CML length, while the path averaged rain rate was decreasing. The five-minute PIA exceedance level (see Figure 3j) was between 10 dB (1st percentile), occurring mostly for shorter CMLs, and 53 dB (99th percentile), occurring mostly for longer CMLs. On average, a path-average rain rate of 42.8 mmh^{-1} and a PIA of 32.7 dB were exceeded for five minutes per year and a rain rate of 17.9 mmh^{-1} and a PIA of 13.5 dB were exceeded for 60 minutes per year.

Using the expected PIA values and our estimates of D_{range} we calculated n_{ex} which is shown in Figure 4b). The majority of D_{range} was between 30dB and 50dB with higher values for longer CMLs (Figure 4a). Even though D_{range} was increasing with length, n_{ex} was also increasing with length.

3.4 Comparison of observed and expected blackouts

The amount of observed blackout minutes per year n_{obs} in relation to each CMLs frequency and length is shown in Figure 4c). We observed that n_{obs} rose with CML length, similar to n_{ex}. Longer CMLs missed a higher percentage of the annual precipitation amount than shorter CMLs (see Figure 2b) and c). According to n_{ex} a 99.99% availability margin (as recommended by the ITU which equals less than 60 minutes of blackouts per year)

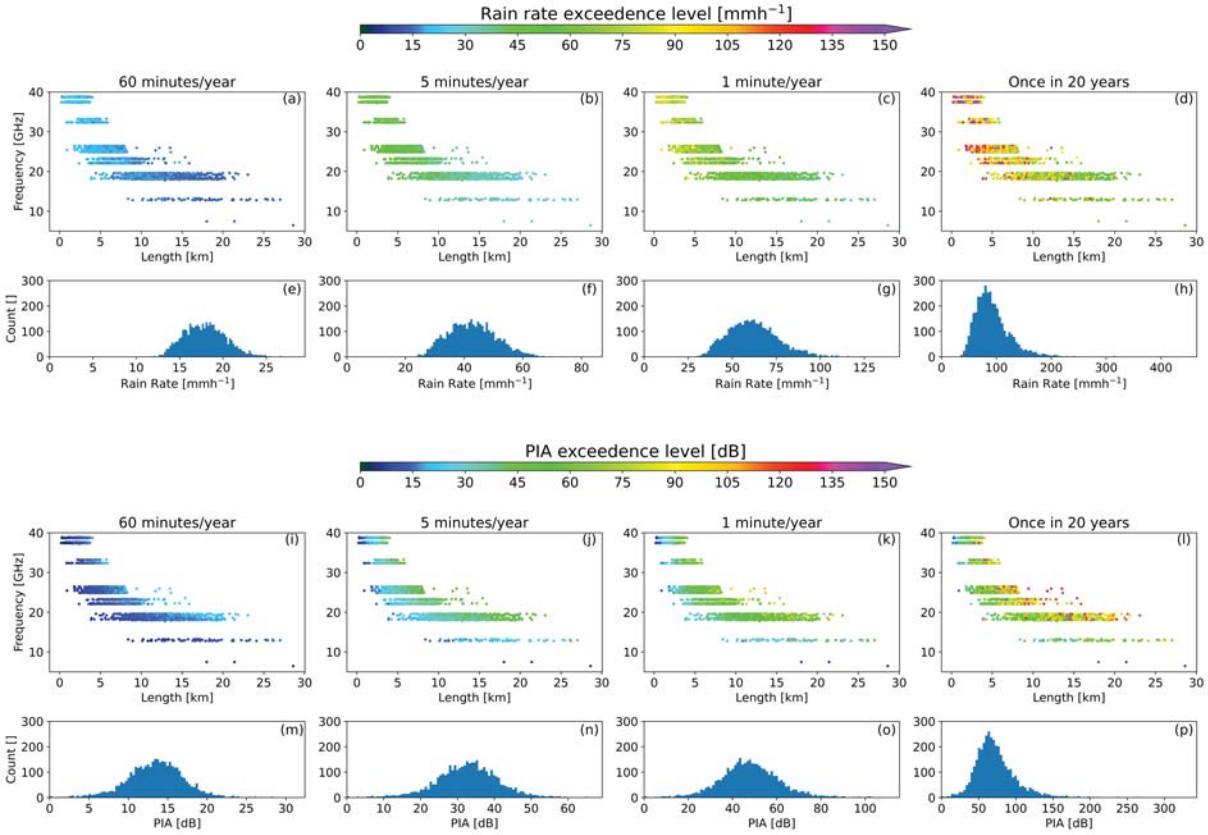

Figure 3. Rainfall and attenuation climatology based on 20 years of RADKLIM-YW. The path-averaged rain rate exceeded along each CML path of a given length and frequency for at least 60, five and one minutes per year and the maximum rain rate occurring once in 20 years are shown in a)-d). Corresponding histograms are given in e)-h). The same climatology for path-integrated attenuation derived via the k-R relation is given in i)-l) and histograms m)-p).

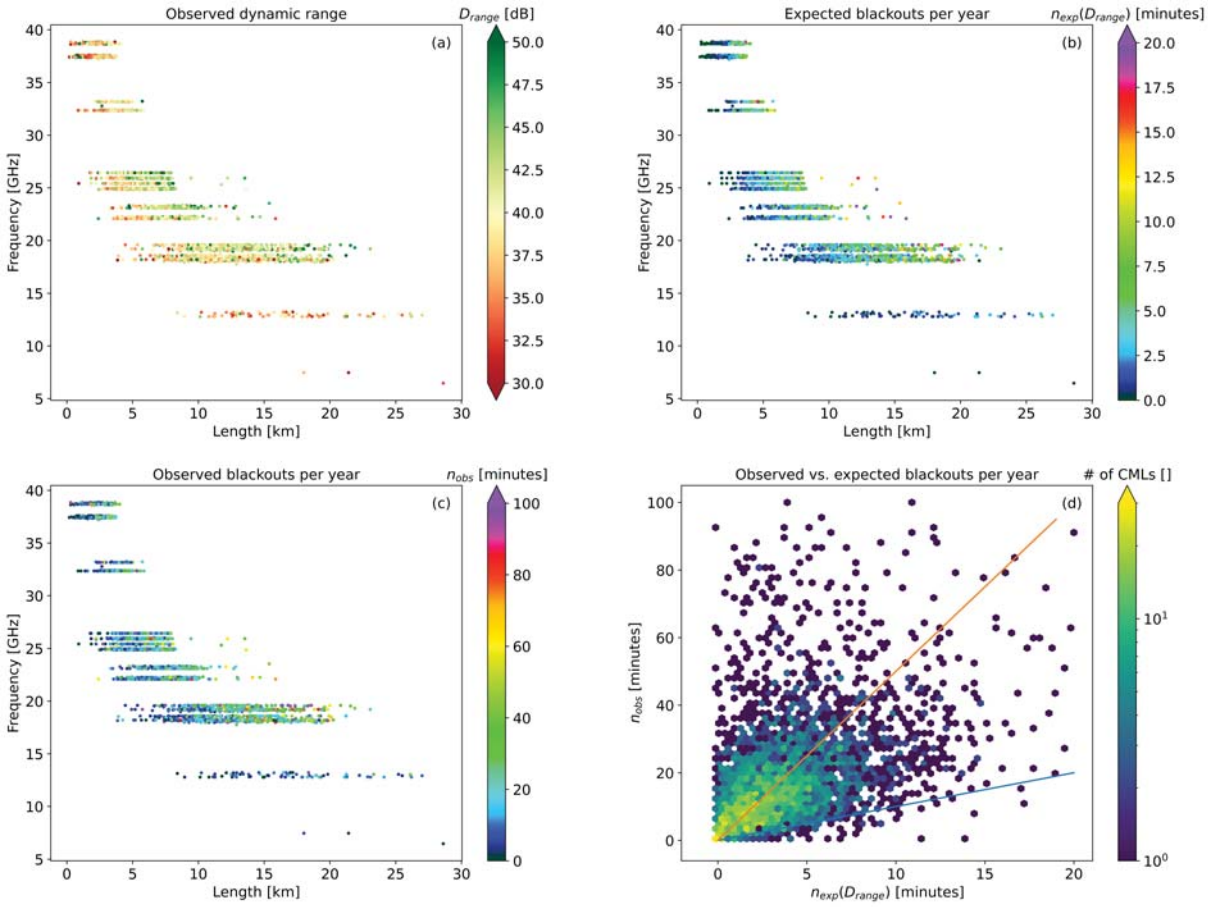

Figure 4. Observed and expected blackout minutes against CML length and frequency. Radar derived path averaged rain rates that exceed the observed D_{range} (see a) lead to an expected number of blackout minutes per year and CML (see b). The observed number of blackout minutes per CML shown in c) is compared to the expected blackout minutes in the scatter density plot d), where the blue line corresponds to a 1:1 relation and the orange line corresponds to a 5:1 relation. Outliers in d), i.e. $n_{obs} > 100$ and $n_{ex} > 20$ are not shown (113 CMLs).

should have been observed for all CMLs. In practice (n_{obs}) the 99.99% margin was exceeded for the longest CMLs in each frequency band.

In Figure 4d), n_{ex} is compared to n_{obs}. On average n_{obs} was twelve times higher than n_{ex} for all CMLs where $n_{ex} > 0$. The average n_{obs} for CMLs where $n_{ex} = 0$ was 19.4. 95.0% of all CMLs showed more observed blackout minutes than expected, i.e. $\frac{n_{obs}}{n_{ex}} > 1$. For 47.6% we observed $\frac{n_{obs}}{n_{ex}} > 5$ and for 22.8% we observed $\frac{n_{obs}}{n_{ex}} > 10$. The 99th percentiles of n_{obs} and n_{ex} were 207.2 and 17.5 minutes which agrees with the average increase of observed against expected blackouts.

4 Discussion

4.1 Effects of CML length on blackout gaps and network design

The result that short CMLs have a lower likeliness to experience a blackout gap than longer CMLs was unexpected, because the dynamic range increases with CML length to account for the increasing PIA. Also, the path-averaging effect results in lower peak

intensities of the path-averaged rain rates which decreases the attenuation per kilometer of CML length.

We found this difference between short and long CMLs in both our CML dataset and our radar-based attenuation climatology. Since observed and expected blackouts are based on independent methodological assumptions, we are confident that the effect is real. One potential explanation is that the path-averaging effect of peak intensities is overestimated during planning of the CMLs availability, so that longer CMLs experience more PIA than expected.

Our findings show potential to improve planning for future CML installations. Most prominently, our results suggest to increase the dynamic range of long CMLs. Our radar-based exceedance probability can be used to estimate the potential increase of blackouts with CML length on the one hand. The total number of blackouts should be expected to be much higher on the other hand, which requires an additional increase of the dynamic range for all CMLs. As the ITU-recommended 99.99% availability was satisfied in most cases, this recommendation may be more urgent for hydrometeorological applications than network stability.

4.2 Implications of blackouts on CML rainfall estimation

Previous studies which compared CML rainfall information against reference data, naturally considered blackouts as missing values and little attention was payed to their implication on CML rainfall estimation. Our results confirmed that their impact on annual precipitation sums is in fact low with around 1% .

However, blackout gaps do impact CML-derived rainfall maps on shorter time scales and extreme value statistics in general, because extreme values are lost. The importance of this effect is illustrated by Figure 2 which shows the occurrence of blackouts during certain radar rainfall rates. The probability of a blackout at path-averaged rainfall intensities beyond 100mm/h is higher than 40%. To interpret such maximum observable path-averaged rainfall rates the path-averaging effect of the CML observation needs to be taken into account, which is different from point-like observations.

Since we observed that shorter CMLs have a much lower probability of blackout gaps, there cannot be a general conclusion about the capability of a CML network to capture rainfall extremes. We can imagine several possibilities to deal with blackouts hampering rainfall estimates. For applications requiring estimates of rainfall maxima on high temporal scales, only short CMLs could be used. Another solution could be to fill RSL during detected blackout gaps with the minimal observable RSL value. Although the true maxima cannot be recovered, this could be a reasonable first step to reduce the considerable underestimation of high rain rates in CML-derived rainfall maps.

4.3 Underestimation of blackouts through radar-based attenuation climatology

Our results also have potential implications for radar rainfall estimates. There were more than ten times more observed blackouts than expected from the radar-based climatology. The underestimation occurs even though our dynamic range estimate is rather conservative due to undersampling of RSL_{min} and the consideration of 3dB WAA. Although false positive blackout detection can not be excluded with certainty, manual checks of the blackout gap detection (see Graf et al. (2022a)) confirmed the correct magnitude of observed blackouts for the vast majority of CMLs.

Therefore, we conclude that radar derived path averaged rain rates and the related PIA underestimate extreme values. This is supported by studies reporting that even gauge adjusted radar products often underestimate heavy rainfall (e.g. (Schleiss et al., 2020)). This underestimation can be explained by the different spatial integration characteristic of CML and radar and the path averaging of the radar along the CML paths. Another reason for the underestimation are effects that occur in combination with rainfall,

e.g. hail, that may lead to unexpected, high attenuation values which may be neglected by weather radar rainfall estimates.

5 Conclusions

During extreme heavy rain events, CMLs may experience blackouts, i.e., complete loss of signal. Our objectives were to determine the impact on rainfall estimation, the occurrence of blackouts in a country-wide network of 3904 CMLs and to determine if these numbers were consistent with the theoretical blackout time derived from a 20-year climatology of a high-resolution weather radar product. On average, CMLs experienced 20 minutes of blackout per year, twelve times more than the radar climatology suggested. Shorter CMLs had fewer blackouts in both the observed and theoretically derived data. Although the amount of rainfall missed was small compared to annual sums, the observed probability of blackouts during path-averaged radar rainfall intensities beyond 100mm/h was more than 40%, which impacts rainfall estimates on short timescales. Especially surprising was the increase of blackouts with CML length. Therefore, we suggest that the CML research community should be aware of this limitation and the proposed mitigation measures. Finally, this study fills a knowledge gap on the distribution of blackouts in CML data and weather radar derived attenuation climatology which can be considered in future CML infrastructure planning.

Acknowledgments

We thank Ericsson, especially Reinhard Gerigk, Michael Wahl, and Declan Forde for their support in the CML data acquisition. This research has been supported by the Helmholtz Association (grant ZT-0025), the German Research Foundation (grant CH-1785/1-2) and the Federal Ministry of Education and Research (grant 13N14826).

Open research

Software for the blackout gap detection routine (Graf et al., 2022a) is available within the CML rainfall retrieval Python-package pycomlink (Chwala et al., 2022) under BSD-3-Clause License. The CML data supporting this research was provided to the authors by Ericsson, restricting the distribution of this data due to their commercial interest. In order to obtain CML data for research purposes a separate and individual agreement with the network provider has to be established. To allow for an independent evaluation of our methodology we published data from 500 CMLs over ten days and two CMLs for the full period of this study (Chwala et al., 2022; Graf et al., 2022b) under CC BY 4.0. The RADKLIM-YW dataset used in this research is publicly available and can be downloaded from Winterrath et al. (2018).

References

Berne, A., & Uijlenhoet, R. (2007). Path-averaged rainfall estimation using microwave links: Uncertainty due to spatial rainfall variability. *Geophysical Research Letters*, *34*(7). Retrieved 2019-03-29, from `https://agupubs.onlinelibrary.wiley.com/doi/abs/10.1029/2007GL029409` doi: 10.1029/2007GL029409

Chwala, C., Keis, F., & Kunstmann, H. (2016, March). Real-time data acquisition of commercial microwave link networks for hydrometeorological applications. *Atmospheric Measurement Techniques*, *9*(3), 991–999. Retrieved 2019-02-22, from `https://www.atmos-meas-tech.net/9/991/2016/` doi: 10.5194/amt-9-991-2016

Chwala, C., & Kunstmann, H. (2019). Commercial microwave link networks for rainfall observation: Assessment of the current status and future challenges. *Wi-*

ley Interdisciplinary Reviews: Water, *6*(2), e1337. Retrieved 2019-02-18, from https://onlinelibrary.wiley.com/doi/abs/10.1002/wat2.1337 doi: 10.1002/wat2.1337

Chwala, C., Polz, J., Graf, M., DanSereb, nblettner, keis f, & yboose. (2022, January). *pycomlink/pycomlink: v0.3.4*. Zenodo. Retrieved 2022-03-09, from https://zenodo.org/record/5832991 doi: 10.5281/zenodo.5832991

Cristiano, E., ten Veldhuis, M.-C., & van de Giesen, N. (2017, July). Spatial and temporal variability of rainfall and their effects on hydrological response in urban areas – a review. *Hydrology and Earth System Sciences*, *21*(7), 3859–3878. Retrieved 2020-12-08, from https://hess.copernicus.org/articles/21/3859/2017/ (Publisher: Copernicus GmbH) doi: https://doi.org/10.5194/hess-21-3859-2017

Ericsson. (2012). *Receiver Performance; Receiver Thresholds Rau1 - Ericsson MINI-LINK E Technical Description [Page 136] | ManualsLib.* Retrieved 2022-02-09, from https://www.manualslib.com/manual/1620197/Ericsson-Mini-Link-E.html?page=136#manual

Fencl, M., Rieckermann, J., Schleiss, M., Stránský, D., & Bareš, V. (2013, October). Assessing the potential of using telecommunication microwave links in urban drainage modelling. *Water Science and Technology*, *68*(8), 1810–1818. Retrieved 2019-04-24, from https://iwaponline.com/wst/article/68/8/1810/17887/Assessing-the-potential-of-using-telecommunication doi: 10.2166/wst.2013.429

Graf, M., Chwala, C., Polz, J., & Kunstmann, H. (2020, June). Rainfall estimation from a German-wide commercial microwave link network: optimized processing and validation for 1 year of data. *Hydrology and Earth System Sciences*, *24*(6), 2931–2950. Retrieved 2020-06-16, from https://www.hydrol-earth-syst-sci.net/24/2931/2020/ (Publisher: Copernicus GmbH) doi: https://doi.org/10.5194/hess-24-2931-2020

Graf, M., El Hachem, A., Eisele, M., Seidel, J., Chwala, C., Kunstmann, H., & Bárdossy, A. (2021, October). Rainfall estimates from opportunistic sensors in Germany across spatio-temporal scales. *Journal of Hydrology: Regional Studies*, *37*, 100883. Retrieved 2021-10-28, from https://www.sciencedirect.com/science/article/pii/S2214581821001129 doi: 10.1016/j.ejrh.2021.100883

Graf, M., Polz, J., & Chwala, C. (2022a, March). *Blackout gap detection example notebook.* Retrieved 2022-03-16, from https://github.com/pycomlink/pycomlink/blob/12fc302539851b19f7656cf7e2438c0ddbaa48bf/notebooks/Blackout%20gap%20detection%20examples.ipynb

Graf, M., Polz, J., & Chwala, C. (2022b, March). *Data for a CML blackout gap detection example.* Zenodo. Retrieved 2022-03-09, from https://zenodo.org/record/6337557 (Type: dataset) doi: 10.5281/zenodo.6337557

Imhoff, R. O., Overeem, A., Brauer, C. C., Leijnse, H., Weerts, A. H., & Uijlenhoet, R. (2020). Rainfall Nowcasting Using Commercial Microwave Links. *Geophysical Research Letters*, *47*(19), e2020GL089365. Retrieved 2022-03-10, from https://onlinelibrary.wiley.com/doi/abs/10.1029/2020GL089365 (_eprint: https://onlinelibrary.wiley.com/doi/pdf/10.1029/2020GL089365) doi: 10.1029/2020GL089365

ITU-R. (2005). *Specific attenuation model for rain for use in prediction methods (Recommendation P.838-3). Geneva, Switzerland: ITU-R. Retrieved from https:// www.itu.int/rec/R-REC-P.838-3-200503-I/en.* Retrieved from https://www.itu.int/rec/R-REC-P.838-3-200503-I/en

ITU-R. (2017). *Characteristics of precipitation for propagation modelling (Recommendation P.837-7). Geneva, Switzerland: ITU-R. Retrieved from https://www.itu.int/rec/R-REC-P.837/en.* Retrieved from https://www.itu.int/rec/R-REC-P.837/en

Leijnse, H., Uijlenhoet, R., & Stricker, J. N. M. (2008, November). Microwave link rainfall estimation: Effects of link length and frequency, temporal sampling, power resolution, and wet antenna attenuation. *Advances in Water Resources*, *31*(11), 1481–1493. Retrieved 2018-12-19, from http://www.sciencedirect.com/science/article/pii/S0309170808000535 doi: 10.1016/j.advwatres.2008.03.004

Overeem, A., Leijnse, H., Leth, T. C. v., Bogerd, L., Priebe, J., Tricarico, D., ... Uijlenhoet, R. (2021, July). Tropical rainfall monitoring with commercial microwave links in Sri Lanka. *Environmental Research Letters*, *16*(7), 074058. Retrieved 2022-01-24, from https://doi.org/10.1088/1748-9326/ac0fa6 (Publisher: IOP Publishing) doi: 10.1088/1748-9326/ac0fa6

Overeem, A., Leijnse, H., & Uijlenhoet, R. (2016, October). Two and a half years of country-wide rainfall maps using radio links from commercial cellular telecommunication networks. *Water Resources Research*, *52*(10), 8039–8065. Retrieved 2018-12-17, from https://agupubs.onlinelibrary.wiley.com/doi/abs/10.1002/2016WR019412 doi: 10.1002/2016WR019412

Polz, J., Chwala, C., Graf, M., & Kunstmann, H. (2020, July). Rain event detection in commercial microwave link attenuation data using convolutional neural networks. *Atmospheric Measurement Techniques*, *13*(7), 3835–3853. Retrieved 2020-12-03, from https://amt.copernicus.org/articles/13/3835/2020/ (Publisher: Copernicus GmbH) doi: https://doi.org/10.5194/amt-13-3835-2020

Schleiss, M., Olsson, J., Berg, P., Niemi, T., Kokkonen, T., Thorndahl, S., ... Pulkkinen, S. (2020, June). The accuracy of weather radar in heavy rain: a comparative study for Denmark, the Netherlands, Finland and Sweden. *Hydrology and Earth System Sciences*, *24*(6), 3157–3188. Retrieved 2021-02-23, from https://hess.copernicus.org/articles/24/3157/2020/ (Publisher: Copernicus GmbH) doi: https://doi.org/10.5194/hess-24-3157-2020

Schleiss, M., Rieckermann, J., & Berne, A. (2013, September). Quantification and Modeling of Wet-Antenna Attenuation for Commercial Microwave Links. *IEEE Geoscience and Remote Sensing Letters*, *10*(5), 1195–1199. doi: 10.1109/LGRS.2012.2236074

Sevruk, B. (2006). Rainfall Measurement: Gauges. In *Encyclopedia of Hydrological Sciences.* John Wiley & Sons, Ltd. Retrieved 2022-01-26, from https://onlinelibrary.wiley.com/doi/abs/10.1002/0470848944.hsa038 (Section: 35 _eprint: https://onlinelibrary.wiley.com/doi/pdf/10.1002/0470848944.hsa038) doi: 10.1002/0470848944.hsa038

Smiatek, G., Keis, F., Chwala, C., Fersch, B., & Kunstmann, H. (2017, March). Potential of commercial microwave link network derived rainfall for river runoff simulations. *Environmental Research Letters*, *12*(3), 034026. Retrieved 2019-07-26, from https://doi.org/10.1088%2F1748-9326%2Faa5f46 doi: 10.1088/1748-9326/aa5f46

Stransky, D., Fencl, M., & Bares, V. (2018, April). Runoff prediction using rainfall data from microwave links: Tabor case study. *Water Science and Technology*, *2017*(2), 351–359. Retrieved 2021-09-15, from https://doi.org/10.2166/wst.2018.149 doi: 10.2166/wst.2018.149

Uijlenhoet, R., Overeem, A., & Leijnse, H. (2018, July). Opportunistic remote sensing of rainfall using microwave links from cellular communication networks. *Wiley Interdisciplinary Reviews: Water*, *5*(4). Retrieved 2018-12-17, from https://onlinelibrary.wiley.com/doi/abs/10.1002/wat2.1289 doi: 10.1002/wat2.1289

van Leth, T. C., Overeem, A., Leijnse, H., & Uijlenhoet, R. (2018, August). A measurement campaign to assess sources of error in microwave link rainfall estimation. *Atmospheric Measurement Techniques*, *11*(8), 4645–4669. Retrieved

2019-02-22, from https://www.atmos-meas-tech.net/11/4645/2018/ doi: 10.5194/amt-11-4645-2018

Winterrath, T., Brendel, C., Hafer, M., Junghänel, T., Klameth, A., Lengfeld, K., ... Becker, A. (2018). Radar climatology (RADKLIM) version 2017.002: Reprocessed quasi gauge-adjusted radar data, 5-minute precipitation sums (YW).
doi: 10.5676/DWD/RADKLIM_YW_V2017.002

Figure 1. Fig1.jpg

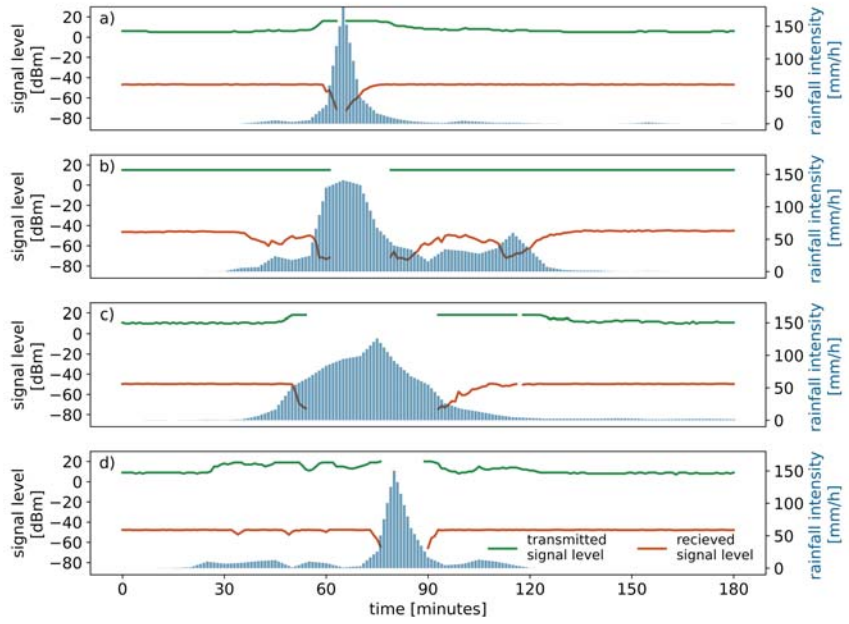
a)
b)
c)
d)
signal level [dBm]
rainfall intensity [mm/h]
transmitted signal level
recieved signal level
time [minutes]

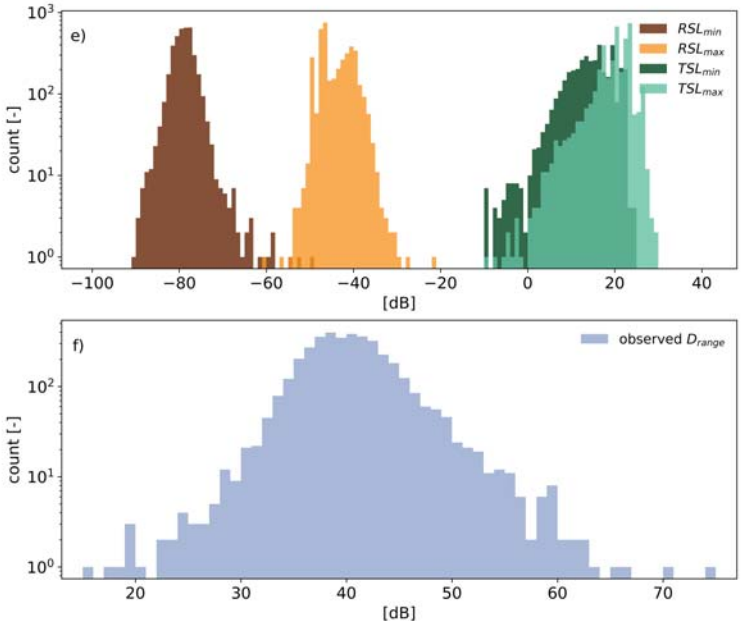
e)
RSL_{min}
RSL_{max}
TSL_{min}
TSL_{max}
count [-]
[dB]
f)
observed D_{range}
count [-]
[dB]

Figure 2.

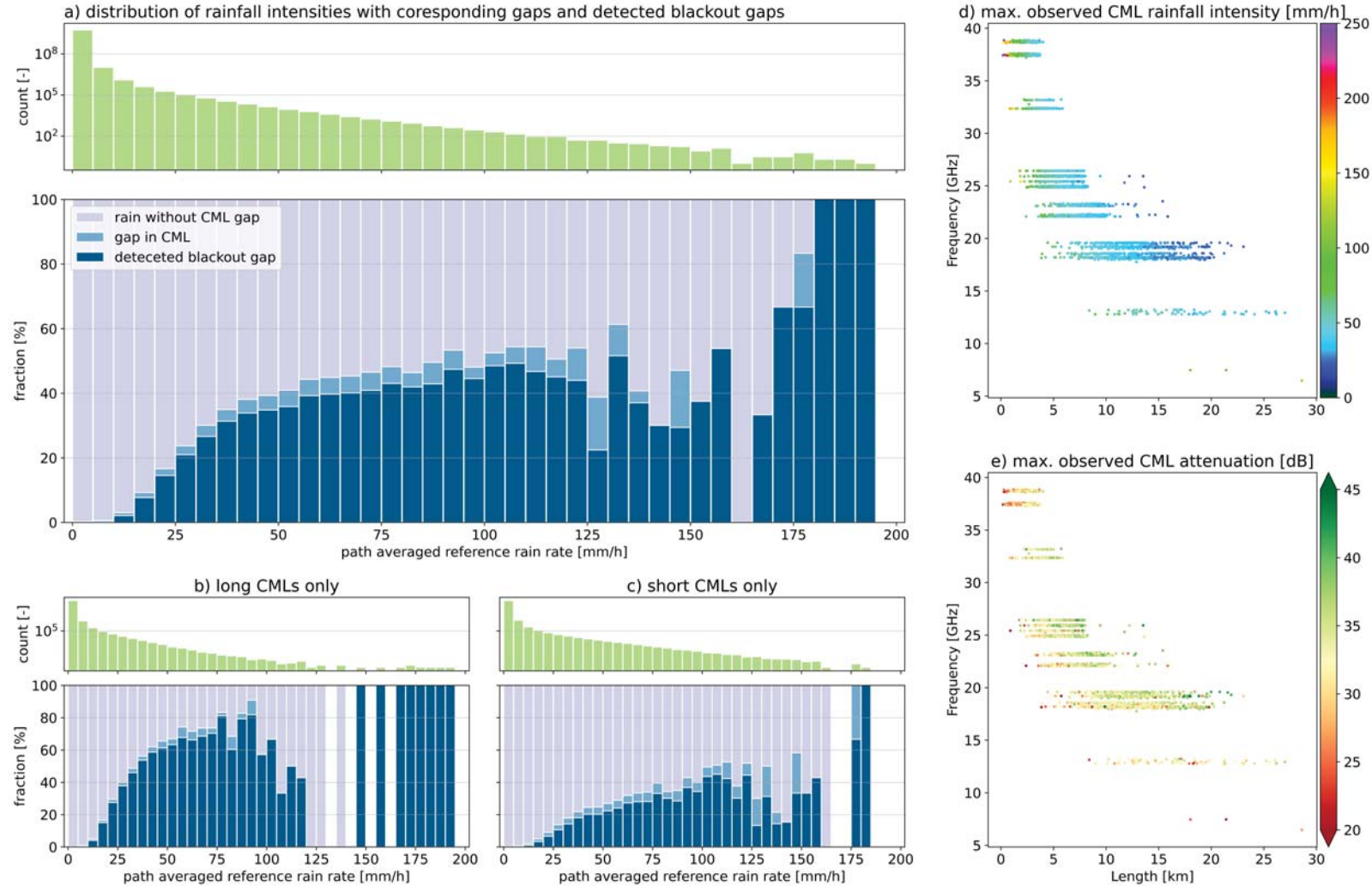
a) distribution of rainfall intensities with coresponding gaps and detected blackout gaps
count [-]
fraction [%]
rain without CML gap
gap in CML
deteceted blackout gap
path averaged reference rain rate [mm/h]
b) long CMLs only
c) short CMLs only
d) max. observed CML rainfall intensity [mm/h]
Frequency [GHz]
e) max. observed CML attenuation [dB]
Length [km]

Figure 3.

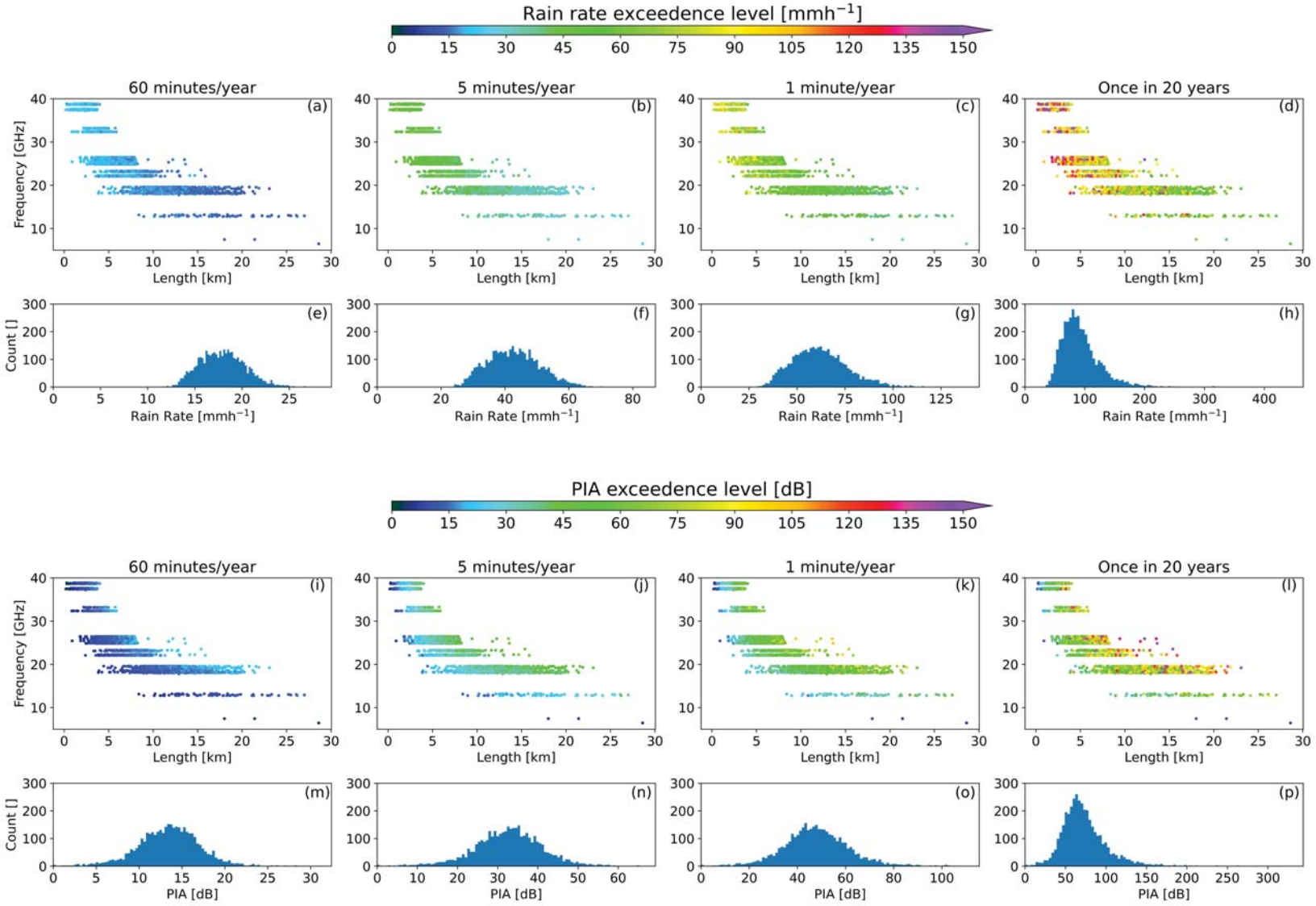
Rain rate exceedence level [mmh^{-1}]
0 15 30 45 60 75 90 105 120 135 150
60 minutes/year
5 minutes/year
1 minute/year
Once in 20 years
(a)
(b)
(c)
(d)
Frequency [GHz]
Length [km]
(e)
(f)
(g)
(h)
Count []
Rain Rate [mmh^{-1}]
PIA exceedence level [dB]
(i)
(j)
(k)
(l)
(m)
(n)
(o)
(p)
PIA [dB]

Figure 4.

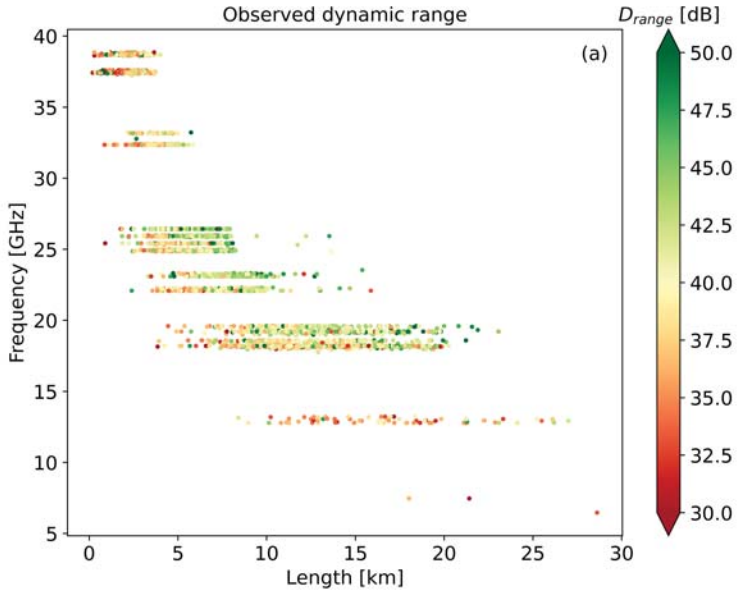
Observed dynamic range
D_{range} [dB]
(a)
Frequency [GHz]
Length [km]

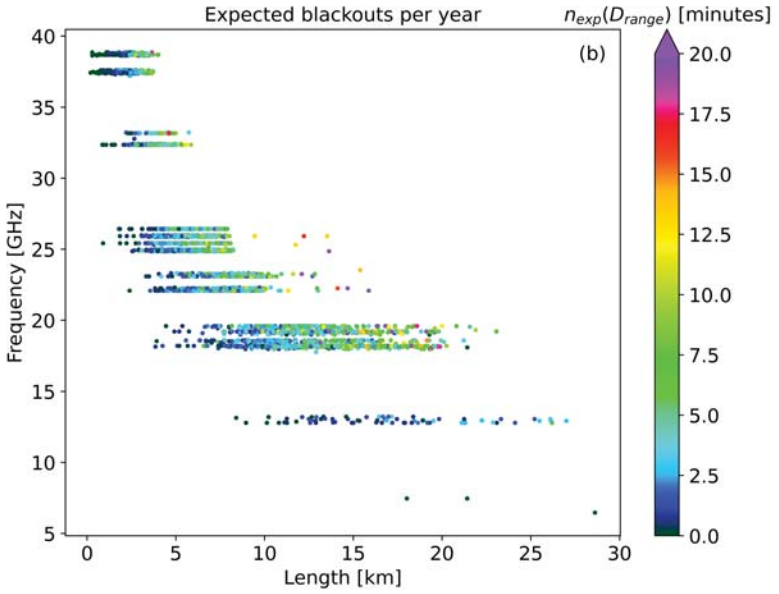
Expected blackouts per year
$n_{exp}(D_{range})$ [minutes]
(b)
Frequency [GHz]
Length [km]

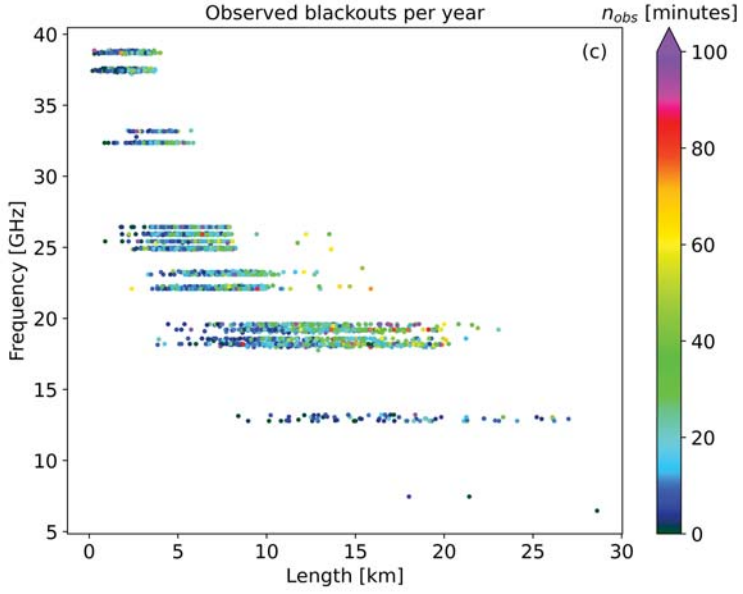
Observed blackouts per year
n_{obs} [minutes]
(c)
Frequency [GHz]
Length [km]

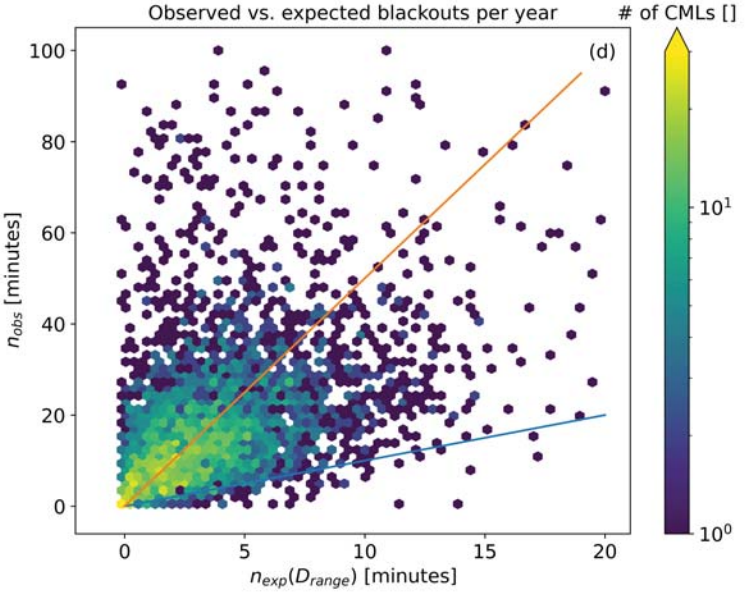
Observed vs. expected blackouts per year
# of CMLs []
(d)
n_{obs} [minutes]
$n_{exp}(D_{range})$ [minutes]